analytical chemistry

pubs.acs.org/ac Article

Rapid ^{13}C Hyperpolarization of the TCA Cycle Intermediate α-Ketoglutarate via SABRE-SHEATH

Isaiah Adelabu, Jessica Ettedgui,* Sameer M. Joshi, Shiraz Nantogma, Md Raduanul H. Chowdhury, Stephen McBride, Thomas Theis, Venkata R. Sabbasani, Mushti Chandrasekhar, Deepak Sail, Kazutoshi Yamamoto, Rolf E. Swenson,* Murali C. Krishna, Boyd M. Goodson, and Eduard Y. Chekmenev*

Cite This: *Anal. Chem.* 2022, 94, 13422−13431 Read Online

ACCESS | Metrics & More | Article Recommendations | Supporting Information

ABSTRACT: α-Ketoglutarate is a key biomolecule involved in a number of metabolic pathways—most notably the TCA cycle. Abnormal α-ketoglutarate metabolism has also been linked with cancer. Here, isotopic labeling was employed to synthesize [1-^{13}C,5-^{12}C,D$_4$]α-ketoglutarate with the future goal of utilizing its [1-^{13}C]-hyperpolarized state for real-time metabolic imaging of α-ketoglutarate analytes and its downstream metabolites *in vivo*. The signal amplification by reversible exchange in shield enables alignment transfer to heteronuclei (SABRE-SHEATH) hyperpolarization technique was used to create 9.7% [1-^{13}C] polarization in 1 minute in this isotopologue. The efficient ^{13}C hyperpolarization, which utilizes parahydrogen as the source of nuclear spin order, is also supported by favorable relaxation dynamics at 0.4 μT field (the optimal polarization transfer field): the exponential ^{13}C polarization buildup constant T_b is 11.0 ± 0.4 s whereas the ^{13}C polarization decay constant T_1 is 18.5 ± 0.7 s. An even higher ^{13}C polarization value of 17.3% was achieved using natural-abundance α-ketoglutarate disodium salt, with overall similar relaxation dynamics at 0.4 μT field, indicating that substrate deuteration leads only to a slight increase (∼1.2-fold) in the relaxation rates for ^{13}C nuclei separated by three chemical bonds. Instead, the gain in polarization (natural abundance versus [1-^{13}C]-labeled) is rationalized through the smaller heat capacity of the "spin bath" comprising available ^{13}C spins that must be hyperpolarized by the same number of parahydrogen present in each sample, in line with previous ^{15}N SABRE-SHEATH studies. Remarkably, the C-2 carbon was not hyperpolarized in both α-ketoglutarate isotopologues studied; this observation is in sharp contrast with previously reported SABRE-SHEATH pyruvate studies, indicating that the catalyst-binding dynamics of C-2 in α-ketoglutarate differ from that in pyruvate. We also demonstrate that ^{13}C spectroscopic characterization of α-ketoglutarate and pyruvate analytes can be performed at natural ^{13}C abundance with an estimated detection limit of 80 micromolar concentration × *%P_{13C}. All in all, the fundamental studies reported here enable a wide range of research communities with a new hyperpolarized contrast agent potentially useful for metabolic imaging of brain function, cancer, and other metabolically challenging diseases.

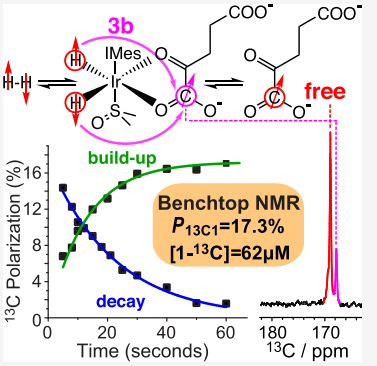

The detection sensitivity of NMR techniques is directly proportional to the degree of nuclear spin alignment of the samples with the applied static magnetic field, *i.e.*, the nuclear spin polarization (P).[1] Because equilibrium P is very low ($\leq 10^{-5}$) even in high-field MRI scanners (*e.g.*, 3 T), MRI is regarded as a low-sensitivity technique in the context of real-time *in vivo* metabolic studies.[2] The advent of nonequilibrium approaches to enhance P far beyond thermal equilibrium all the way to the order unity allows boosting NMR sensitivity by 4+ orders of magnitude (also termed *hyper*polarization), thereby enabling *in vivo* tracking of relatively dilute metabolites (0.1−10 mM), such as [1-^{13}C]pyruvate,[3] [1-^{13}C]lactate,[4] [^{13}C]bicarbonate,[5] and other hyperpolarized (HP) ^{13}C injectable biocompatible molecules.[6] The ^{13}C carboxylic nucleus offers long T_1 (on the order of 1 minute), therefore enabling *in vivo* tracking for up to several minutes.[7] One hyperpolarization technology, dissolution dynamic nuclear polarization (d-DNP),[8] is already under investigation in 29 clinical trials (www.clinicaltrials.gov) to identify the efficacy of HP ^{13}C MRI for detecting aberrant metabolism of HP [1-^{13}C]pyruvate in diseases.[9] Despite the success of d-DNP in research settings to be able to provide safe, injectable HP ^{13}C contrast agents for clinical utilization, this technology has a number of limitations, including high device cost (>$2M) and slow production speed (≥1 h for clinical device) that potentially pose a barrier to translation for widespread clinical

Received: May 18, 2022
Accepted: September 9, 2022
Published: September 22, 2022

use.[10] Lower cost and higher throughput hyperpolarization techniques are desirable to address these challenges.[11,12]

An alternative group of HP techniques that have been developed over the years relies on parahydrogen (p-H_2) as a source of hyperpolarization.[13] Historically, parahydrogen-induced polarization (PHIP)[13,14] relying on pairwise p-H_2 addition was developed first and translated to *in vivo* application approximately 15 years after the initial *in vitro* demonstration.[15] Because this approach relies on the use of a PHIP catalyst required for p-H_2 pairwise addition, it needs to be removed prior to potential clinical use. Moreover, hydrogenation reactions can be performed directly in aqueous media[16,17] to facilitate biocompatible contrast agent preparation. Alternatively, hydrogenation in organic solvents followed by reconstitution into biocompatible aqueous buffer media has also been demonstrated.[18−20] A wide range of biocompatible HP molecular probes has been developed and translated *in vivo*[21−24] using this technique, including most prominently HP [1-^{13}C]pyruvate[25] via a PHIP variant involving side-arm hydrogenation (PHIP-SAH). The key advantages of the PHIP-SAH approach are fast hyperpolarization times (<1 min) and low cost of HP hardware. The key limitation of this method is the requirement of chemical modification of the to-be-hyperpolarized substrate through hydrogenation reactions as well as the need for additional chemical de-esterification of the side arm after ^{13}C nuclei have been hyperpolarized.[12,26,27]

Signal amplification by reversible exchange[28] in shield enables alignment transfer to heteronuclei (SABRE-SHEATH)[29] is an alternative technique to create HP [1-^{13}C]pyruvate.[30,31] This method relies on simultaneous exchange of p-H_2 and a to-be-hyperpolarized substrate (*e.g.*, [1-^{13}C]pyruvate) with a metal complex (*e.g.*, Ir−IMes hexacoordinate complex, *e.g.*, **3b** in Scheme 1) to enable spontaneous polarization transfer from p-H_2-derived hydrides to spin−spin-coupled heteronuclei (*e.g.*, ^{13}C of [1-^{13}C]-pyruvate[30,31]). SABRE-SHEATH was first demonstrated for ^{15}N[29] and then quickly expanded to ^{13}C,[32] ^{19}F,[33] ^{31}P,[34] and other nuclei. In 2019, Duckett and co-workers demonstrated the feasibility of SABRE-SHEATH hyperpolarization of [1-^{13}C]pyruvate using DMSO as a coligand, but ^{13}C polarization levels were limited to 1.85%.[30,35] The addition of DMSO leads to the formation of SABRE-active complex and **3b** (Scheme 1); note that axial positions are not exchanging on the time scale of the SABRE-SHEATH experiment, and therefore, only complex **3b** undergoes an effectively reversible exchange with the HP substrate. The key advantages of the SABRE-SHEATH hyperpolarization approach are the low cost of HP hardware (<$20k) and a rapid (∼1 min) hyperpolarization process.[36] Moreover, this HP technique does not modify the to-be-HP substrate.[37,38] Since HP [1-^{13}C]pyruvate is the leading HP contrast agent, the reader is reminded that d-DNP performs hyperpolarization of [1-^{13}C]pyruvic acid, which is chemically modified to sodium [1-^{13}C]pyruvate via a neutralization reaction. The key limitation of SABRE is that it is most efficient in alcohol solutions, *e.g.*, in methanol, which has poor biocompatibility.[12] Pioneering efforts to produce aqueous solutions of HP compounds via SABRE have improved this issue but so far have led to a marked (by an order of magnitude or more) *P* decrease.[39−44] Development of biocompatible formulations for agents hyperpolarized via SABRE technology remains a key unaddressed translational need, which is outside the scope of this manuscript. The reader is also directed to several recent reviews for detailed descriptions of leading HP technologies.[9,12,26,27,45,46]

We and others have recently demonstrated a series of innovations (including the use of water as an additional potential coligand[47,48] and temperature cycling[37,49]), demonstrating that catalyst-bound [1-^{13}C]pyruvate ^{13}C polarization (P_{13C}) may reach order-unity values,[47] and ^{13}C bulk P_{13C} of up to 13% can be obtained.

The work presented here aims to expand efficient SABRE-SHEATH hyperpolarization to other biologically relevant ketocarboxylic acids, exemplified by α-ketoglutarate. α-Ketoglutarate is a central intermediate of the tricarboxylic acid cycle and other important metabolic pathways.[52] Moreover, HP [1-^{13}C]α-ketoglutarate ([1-^{13}C]α-KG) prepared by d-DNP has been successfully employed to delineate altered metabolism in the isocitrate dehydrogenase 1 (IDH1) gene mutant. Therefore, HP [1-^{13}C]α-KG can inform on IDH1 status via detection of the metabolic product HP [1-^{13}C]2-hydroxyglutarate ([1-^{13}C]2HG), which is missing in wild-type cells.[53] IDH1 mutants are potentially druggable.[53] Accordingly, HP ^{13}C MRI with HP [1-^{13}C]α-KG can inform on IDH1 mutation and thus has the potential to guide cancer patient treatment.[53]

A pioneering study employing HP [1-^{13}C]α-ketoglutarate showed that the HP resonance of the metabolic product [1-^{13}C]2HG may overlap with the natural-abundance HP resonance from the ^{13}C-5 carbon of [1-^{13}C]α-KG. To mitigate this potential translational challenge of spectral overlap, Miura and co-workers have recently synthesized [1-^{13}C,5-^{12}C]α-KG and employed this HP isotopologue for detecting HP [1-^{13}C]2HG in IDH1 mutants without a natural-abundance HP ^{13}C-5 background signal.[54] Taglang and co-workers have also demonstrated that late-stage deuteration of HP carboxylic acids can extend carboxylate ^{13}C T_1 by up to a factor of 4.[55] That work indicated that ^{13}C HP metabolic probes or *in vivo* analytes could generally benefit from deuteration to improve the lifetime of the ^{13}C HP state of the molecular probe.[55]

Inspired by the previous works, we have synthesized [1-^{13}C,5-^{12}C,D$_4$]α-KG, as shown in Scheme 2. Here, we have hyperpolarized two α-KG isotopologues to study their utility

Scheme 1. Formation of [IrCl(H)$_2$(DMSO)$_2$(IMes)] (2) and [Ir(H)$_2$(η2-substrate)(DMSO)(IMes)] (3) Complexes Following Activation of [IrIMes(COD)Cl] (1) precatalyst[a]

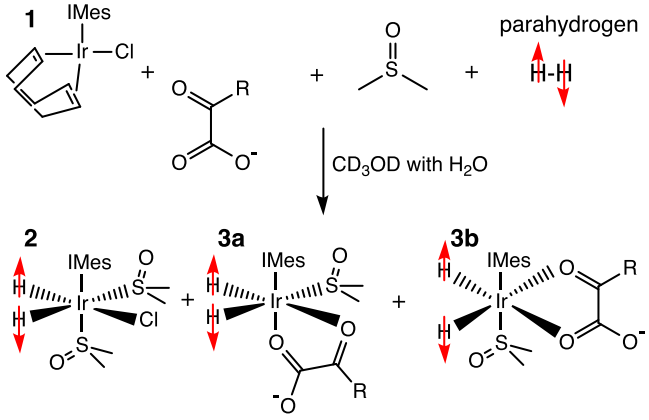

[a]Catalyst 1 was prepared previously[50] according to Cowley et al.[51] Species **1**, **2**, **3a**, and **3b** are as indicated by Iali et al. for pyruvate variants.[30] R = CH_3 for pyruvate and R = CH_2-CH_2-COO^- for α-KG.

https://doi.org/10.1021/acs.analchem.2c02160
Anal. Chem. 2022, 94, 13422−13431

Scheme 2. Overall Synthetic Schematic of [1-^{13}C,5-^{12}C,D$_4$]α-KG[a]

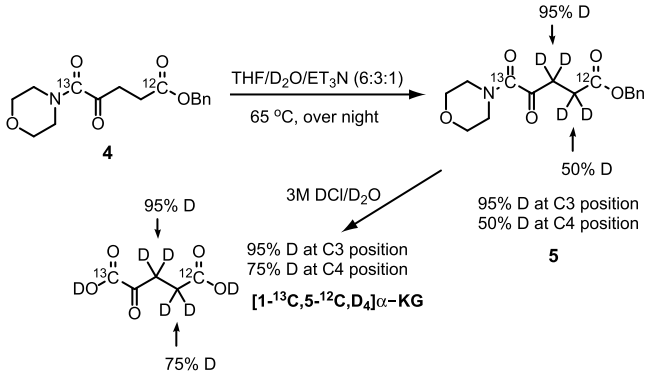

[a]See the Supporting Information (SI) for details of the experimental procedure and characterization details.

for SABRE-SHEATH: natural-abundance α-KG and newly developed [1-^{13}C,5-^{12}C,D$_4$]α-KG depicted in Scheme 1.

MATERIALS AND METHODS

The standard precatalyst used for SABRE [IrCl(COD)(IMes)] (IMes = 1,3-bis(2,4,6-trimethylphenyl)imidazol-2-ylidene; COD = cyclooctadiene),[51,56] and catalyst **1** (6 mM) was activated with p-H$_2$ bubbling in the presence of ∼5 mM α-KG, 20 mM DMSO, and 0.5 M H$_2$O in CD$_3$OD (Figure 1, **top**), corresponding to our previously optimized protocol for preparation of HP [1-^{13}C]pyruvate (P_{13C} = 13%).[47] We used a low α-KG concentration (5 mM) because of the low α-KG solubility in CD$_3$OD. Fast activation (<5 min) leads to the formation of species **2**, **3a**, and **3b** in accord with the notation introduced by Duckett and co-workers (in the context of pyruvate SABRE).[30,31] Complex **3b** is the primary SABRE-active species as discussed above. For natural-abundance substrate studies, we have also performed a comparative study with pyruvate.

^{13}C SABRE-SHEATH experiments were performed similarly to the recently reported study for [1-^{13}C]pyruvate[47] by bubbling >98.5% p-H$_2$[57] at a flow rate of 70 standard cubic centimeters per minute (sccm) at a p-H$_2$ partial pressure of 8 atm for 2 min. Parahydrogen was temporarily stored (1−4 days) in aluminum cylinders using the storage and distribution system described in detail in the SI. ^{13}C signal detection was performed using a clinically relevant 1.4 T field. The thermally polarized sample of neat (∼17.5 M) [1-^{13}C]acetic acid (Figure 1d) was employed as a signal reference to compute ^{13}C polarization enhancement and P_{13C} (see the SI).

RESULTS AND DISCUSSION

Simultaneous exchange of p-H$_2$ and α-KG leads to hyperpolarization of the 1-^{13}C site detected in both isotopologues (Figures 1 and 2a,b). The temperature sweep (Figures 1c,g and 2f) reveals that at cold temperatures (*e.g.*, −12 °C), HP species **3b** dominates the spectral intensity. The HP free (*i.e.*, not catalyst bound) is negligible compared to the HP **3b** resonance because the substrate exchange is too slow on the time scale of the experiment.[47] SABRE-SHEATH polarization at an elevated temperature leads to the rise of the resonances from HP-free species with an optimal polarization transfer temperature T_T of 6−10 °C (Figures 1g and 2f) for both isotopologues studied. At this temperature, the exchange rate of the substrate is likely matched to the size of the spin−spin coupling between the parahydrogen-derived hydrides and the ^{13}C-1 nucleus. A field sweep revealed a P_{13C} maximum at B_T of ∼0.42 μT (Figures 1f and 2g).

The high P_{13C} level allows detecting dilute biomolecules with a high SNR at natural ^{13}C abundance (*ca.* 1.1%) even using a benchtop NMR spectrometer, which is remarkable as it substantially expands the capability of the demonstrated approach to potentially screen a wide range of new metabolic analytes that could be amenable to NMR hyperpolarization. Indeed, Figure 2b shows a spectrum of HP α-KG with a corresponding signal reference spectrum (neat [1-^{13}C]acetic acid) shown in Figure 2c. We estimate the detection limit of 5 μM at the reported polarization level or ∼80 μM*% polarization of ^{13}C.

Just like in Figure 1, the microtesla relaxation dynamics of the ^{13}C-1 carbon of the naturally abundant isotopologue (Figure 2d) shows that the total P_{13C} (bound+free) buildup time (T_b = 12.8 ± 0.5 s) is substantially shorter than the corresponding T_1 value of 22.4 ± 0.8 s, indicating that the P_{13C} buildup rate substantially exceeds the rate of spin polarization destruction via T_1 relaxation (note the bound **3b** and free species likely have different intrinsic ^{13}C T_1 values mostly because the catalyst itself is a relaxation agent), but since their exchange rate is substantially faster than $1/T_1$, one should observe "the same" average ^{13}C T_1 for both lines that would be weighted by the mole fractions of each site under some set of conditions—hence, the current simplified analysis of our relaxation data. These favorable relaxation dynamics fundamentally enable relatively high P_{13C} levels. Indeed, P_{13C} of up to 17.3% was observed for natural-abundance α-KG (Figure 2b). Somewhat lower maximum P_{13C} values were observed for [1-^{13}C,5-^{12}C,D$_4$]α-KG (*e.g.*, Figure 1b) even though the relaxation dynamics at B_T = 0.42 μT is effectively similar in the labeled isotopologue (T_b = 11.0 ± 0.4 s and T_1 = 18.5 ± 0.8 s, respectively, Figure 1e). Instead, we explain the P_{13C} increase in the naturally abundant isotopologue in terms of the smaller heat capacity of the "spin bath" comprising available ^{13}C spins that must be hyperpolarized by the same number of p-H$_2$ spins.[58] Indeed, the corresponding ^{15}N SABRE-SHEATH studies with isotopically enriched metronidazole and natural-abundance metronidazole revealed substantially greater P_{15N} in the naturally abundant compound[59,60] versus fully labeled analogue.[61,62] Future work on improving p-H$_2$ access to the polarization transfer complex may potentially yield much better P_{13C} levels in HP [1-^{13}C,5-^{12}C,D$_4$]α-KG.

The observation of similar ^{13}C-1 T_b and T_1 values measured at 0.42 μT of the two α-KG isotopologues is also remarkable in the context of exchangeable substrate deuteration. Deuterium is a quadrupolar nucleus that may potentially act as a source of relaxation for the nearby spins due to enhanced scalar relaxation of the second kind.[31,63,64] Therefore, potentially deleterious effects of deuterium on ^{13}C-1 T_1 (and by extension, on the maximum attainable P_{13C-1} due to the increased rate of spin destruction) may be expected in a manner similar to that observed for ^{15}N T_1 relaxation arising from ^{15}N−^{14}N two-bond interactions (where ^{14}N spins act as quadrupolar relaxation sinks).[62] We rationalize the above observation by the negligible strength of the relevant interactions over three (^{13}C-C-C-D) chemical bonds. Indeed, the corresponding ^{15}N-C-C-^{14}N three-bond interactions have also been shown to be too weak to have a measurable effect of microtesla ^{15}N relaxation in SABRE-SHEATH.[65]

https://doi.org/10.1021/acs.analchem.2c02160
Anal. Chem. 2022, 94, 13422−13431

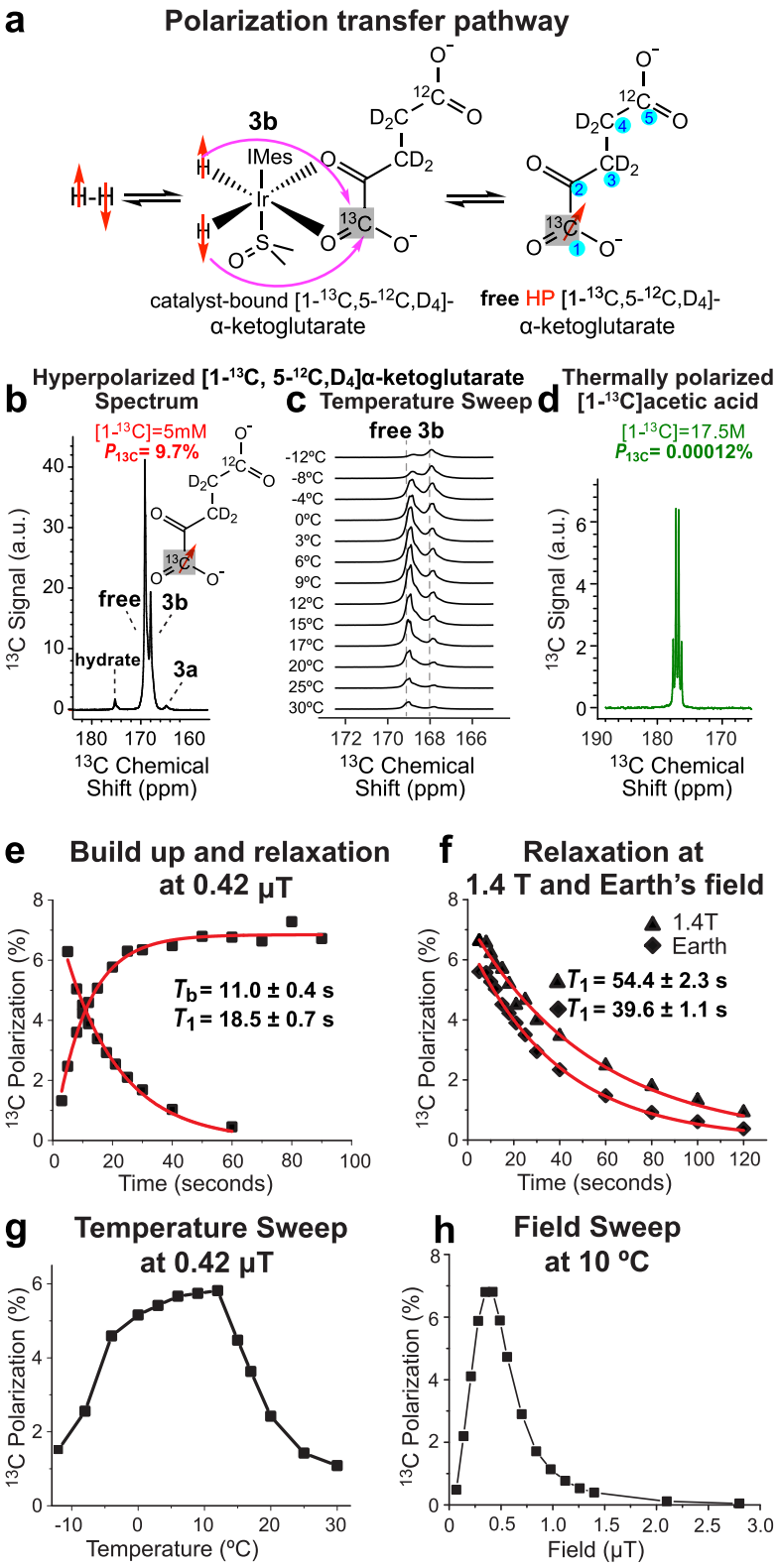

Figure 1. (a) Schematic of the SABRE-SHEATH hyperpolarization process and relevant polarization transfer path of [1-^{13}C,5-^{12}C,D$_4$]α-KG. (b) ^{13}C spectrum of HP [1-^{13}C,5-^{12}C,D$_4$]α-KG; carbon positions are labeled by blue numerals. (c) Representative stacked variable-temperature ^{13}C spectra of 5 mM [1-^{13}C,5-^{12}C,D$_4$]α-KG, demonstrating the interplay between the HP complex **3b** and the "free" peak as a function of temperature during the SABRE-SHEATH hyperpolarization process; (d) corresponding ^{13}C spectrum of thermally polarized neat [1-^{13}C]acetic acid employed as a signal reference for computation of signal enhancements. (e) Buildup and decay of total ^{13}C polarization of ^{13}C-1 (*i.e.*, integrating over all bound and free resonances) in [1-^{13}C,5-^{12}C,D$_4$]α-KG at B_T = 0.42 μT and (f) corresponding ^{13}C-1 T_1 relaxation curves at the Earth's field and the clinically relevant 1.4 T field of the benchtop spectrometer. Total ^{13}C polarization of ^{13}C-1 in [1-^{13}C,5-^{12}C,D$_4$]α-KG as a function of temperature (g) and magnetic transfer field (h). All experiments are performed at 1.4 T using a SpinSolve NMR spectrometer in CD$_3$OD at T_T = +10 °C (unless otherwise noted).

https://doi.org/10.1021/acs.analchem.2c02160
Anal. Chem. 2022, 94, 13422−13431

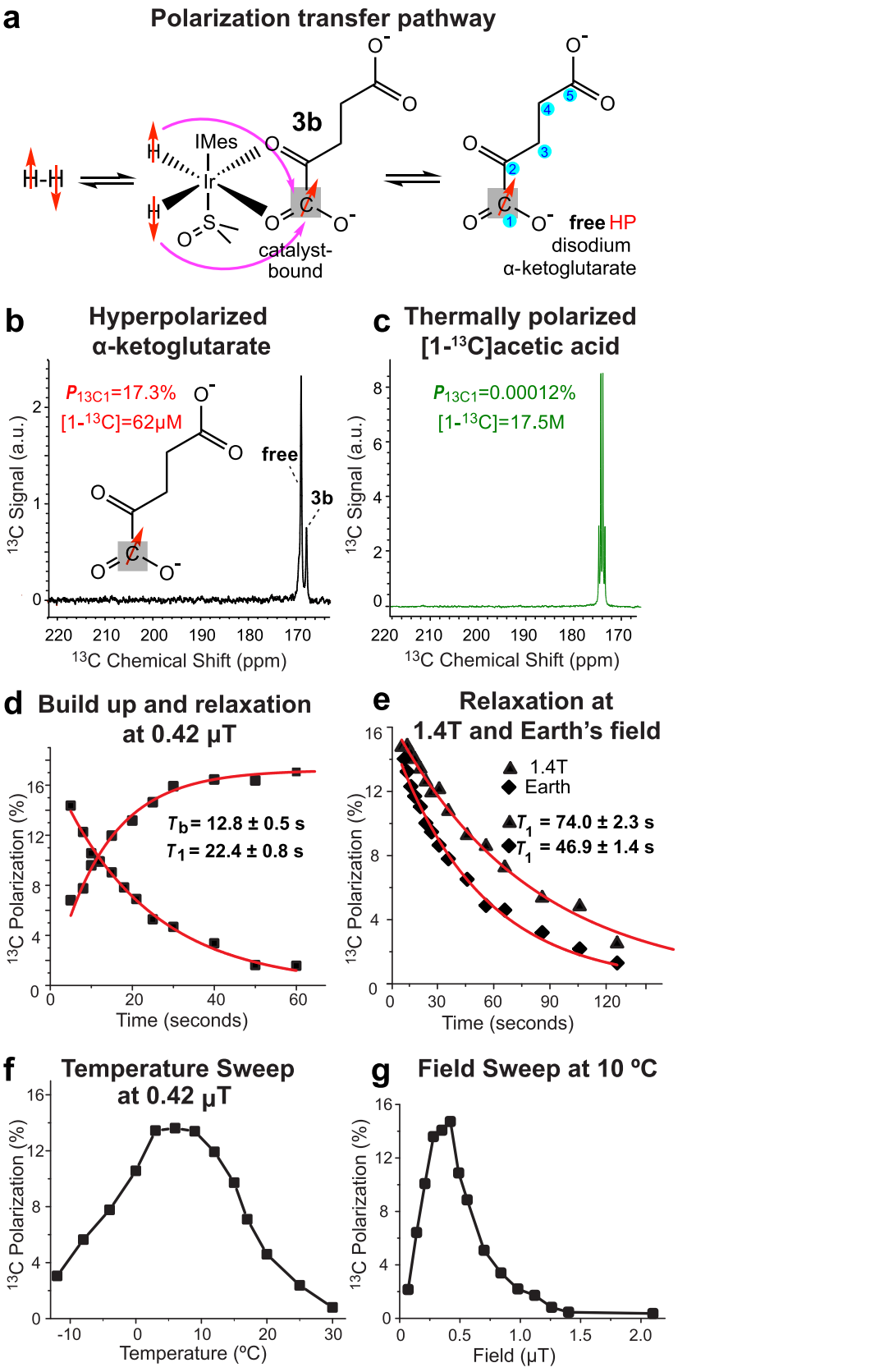

Figure 2. (a) Schematic of the SABRE-SHEATH hyperpolarization process and relevant polarization transfer path of natural-abundance α-KG; carbon positions are labeled by blue numerals. (b) Representative HP ^{13}C spectrum of 5.6 mM natural-abundance α-KG obtained by performing SABRE-SHEATH at +10 °C in CD_3OD at 1.4 T; (c) corresponding ^{13}C spectrum of thermally polarized neat [1-^{13}C]acetic acid; (d) total (bound + free) ^{13}C polarization buildup and decay at B_T = 0.42 μT and T_T = + 10 °C; and (e) total (bound + free) ^{13}C polarization decay at the Earth's field and 1.4 T. Total ^{13}C polarization of ^{13}C-1 in natural-abundance α-KG as a function of (f) temperature and (g) magnetic transfer field. All experiments are performed at 1.4 T using a SpinSolve NMR spectrometer in CD_3OD.

https://doi.org/10.1021/acs.analchem.2c02160
Anal. Chem. 2022, 94, 13422−13431

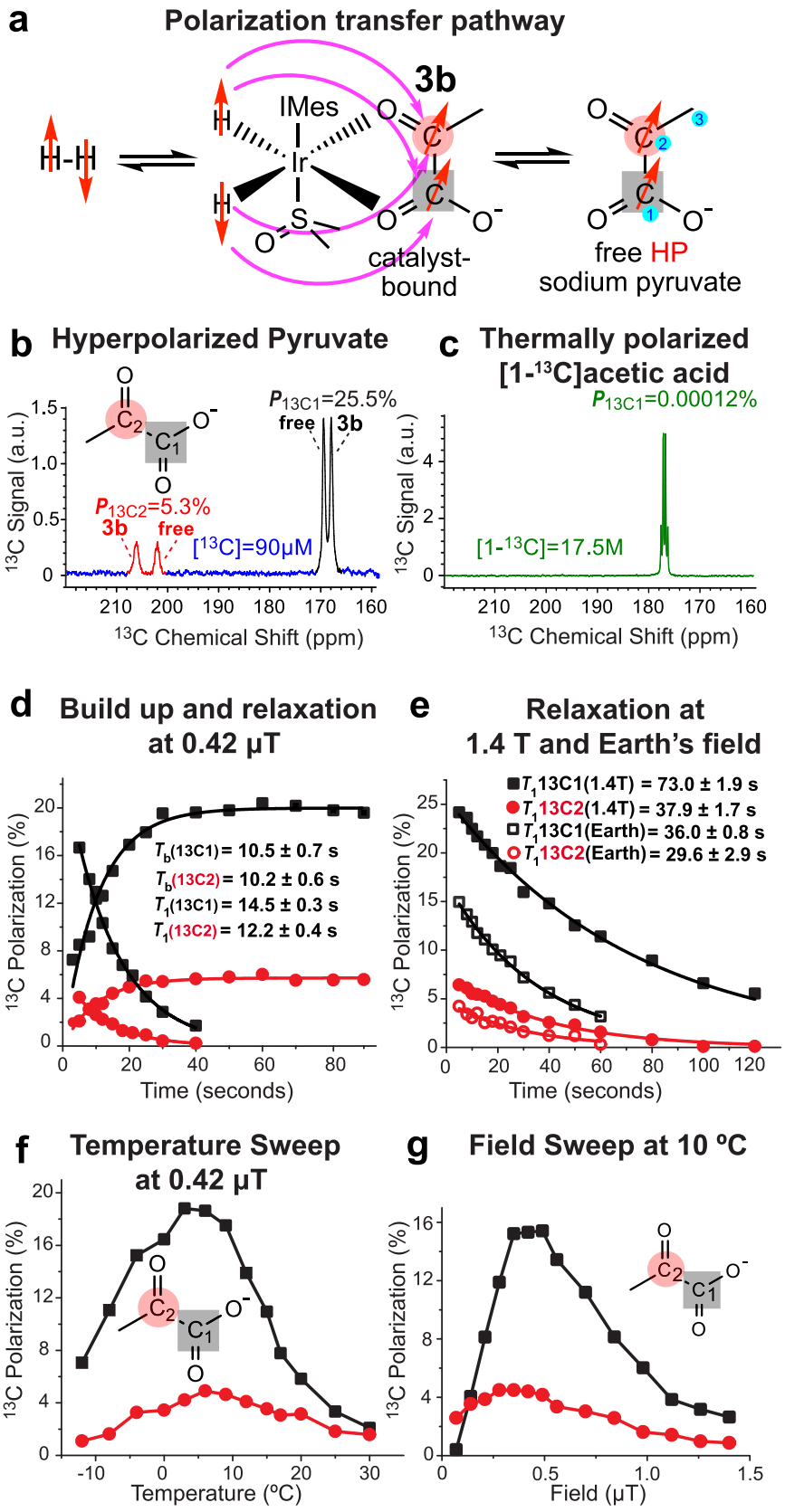

Figure 3. (a) Schematic of the SABRE-SHEATH hyperpolarization process and relevant polarization transfer path of natural-abundance sodium pyruvate; carbon positions are labeled by blue numerals. (b) Representative HP ^{13}C spectrum of 8.6 mM natural-abundance sodium pyruvate obtained by performing SABRE-SHEATH at +10 °C in CD_3OD at 1.4 T; (c) corresponding ^{13}C spectrum of thermally polarized neat [1-^{13}C]acetic acid; (d) total (bound + free) ^{13}C polarization buildup and decay at B_T = 0.42 μT and T_T = +10 °C; and (e) total (bound + free) ^{13}C polarization decay at the Earth's field and 1.4 T. Total ^{13}C polarization of ^{13}C-1 in sodium pyruvate as a function of (f) temperature and (g) magnetic transfer field. All experiments are performed at 1.4 T using a SpinSolve NMR spectrometer in CD_3OD.

https://doi.org/10.1021/acs.analchem.2c02160
Anal. Chem. 2022, 94, 13422−13431

This observation of only a minor effect of γ-position deuteration on ^{13}C-1 T_1 relaxation is important in the context of attaining high ^{13}C-1 polarization levels because it implies that such substrate deuteration may cause no undesirable rapid 1-^{13}C-1 depolarization in microtesla magnetic fields (and by extension, may not interfere with achieving high P_{13C-1} values because the spin destruction rate remains lower than the polarization buildup rate). On the other hand, substrate deuteration will likely have a positive impact on extending 1-^{13}C T_1 in α-KG at clinically relevant magnetic fields (particularly in the absence of the SABRE catalyst).[55] Of note, ^{13}C-1 T_1 values (*e.g.*, 54.4 ± 2.3 s at 1.4 T and 39.6 ± 1.1 s at the Earth's field, Figure 1f) are likely limited by the interplay of the iridium-catalyst-induced and exchange-induced T_1 relaxation processes. This notion is supported by the substantially longer ^{13}C-1 T_1 values even at the higher (and more clinically relevant) 3 T field and in aqueous media (with no SABRE catalyst), *e.g.*, 97.1 ± 0.4 s for [1-^{13}C,5-^{12}C,D$_4$]α-KG; note that the nondeuterated isotopologue yields substantially lower ^{13}C-1 T_1 at 3 T of 63.0±0.8 s, clearly demonstrating the potential clinical translation benefit of substrate deuteration for HP metabolic ^{13}C studies.

We also note that ^{13}C T_1 values at the Earth's field and higher fields are substantially greater than those at the submicrotesla magnetic fields employed here for polarization buildup as part of the (static-field) SABRE-SHEATH process. Therefore, other polarization transfer approaches operating at higher magnetic fields (including but not limited to LIGHT-SABRE,[66] SLIC-SABRE,[67] QUASR-SABRE-SHEATH,[68] pulsed SABRE-SHEATH,[69] alt SABRE-SHEATH,[70] etc.[71,72]) may potentially perform polarization buildup with overall lower ^{13}C T_1 losses and thus may yield overall higher P_{13C} values; future work is certainly warranted in this direction.

Remarkably, no resonance from the HP ^{13}C-2 carbon was detected from either isotopologue (expected between 200 and 210 ppm, see, *e.g.*, the spectrum in Figure 2b). This observation is somewhat unexpected because the spin−spin couplings between parahydrogen-derived hydrides and the ^{13}C-2 site are overall expected to be similar to those of the ^{13}C-1 site (Figure 2a). Moreover, no HP ^{13}C-5 resonance was observed either, suggesting that catalyst coordination with the other carboxyl group does not take place. Prompted by this unexpected lack of ^{13}C-2 hyperpolarization in both α-KG isotopologues, we have performed corresponding studies with natural-abundance pyruvate at a similar (8.6 mM) pyruvate concentration and otherwise the same sample preparation and experimental conditions (Figure 3).

Figure 3b shows the spectrum of HP pyruvate with P_{13C-1} of 25.5% and P_{13C-2} of 5.3%, indeed revealing a remarkable difference in the polarization values of the two binding sites (Figure 3a). The systematic temperature sweeping of the SABRE-SHEATH polarization conditions (Figure 3f) shows a nearly identical position of the maximum for P_{13C-1} and P_{13C-2} at 6−10 °C. Moreover, the microtesla magnetic field sweep (Figure 3f) revealed that optimum B_T for ^{13}C-2 is slightly smaller (∼0.28 μT) versus that for ^{13}C-1 (∼0.42 μT), indicating that the spin−spin interactions between p-H$_2$-derived hydrides and ^{13}C-2 are ∼1.5 times weaker than those for the ^{13}C-1 site. Furthermore, the relaxation analysis of pyruvate ^{13}C-1 and ^{13}C-2 sites at 0.42 μT reveals no substantial differences between the two sites, indicating that the minute difference in the rates of polarization buildup and decay for the two molecular sites during the SABRE-SHEATH process cannot explain the remarkable four- to fivefold difference in P_{13C-1} and P_{13C-2}. It should also be noted that the studies at the natural ^{13}C abundance level allow probing all ^{13}C sites independently due to the low probability (1.1%) of having ^{13}C in both positions at the same time. Taking together the key presented observations, we hypothesize that ^{13}C-2 in pyruvate coordinates the iridium complex (Figure 3a) weaker due to side-chain dynamics induced by the −CH$_3$ group, and as a result, the residence lifetime of the bound ^{13}C-2 site on the catalyst may be reduced, in turn resulting in reduced P_{13C} and lower value of optimal B_T. In the case of α-KG, the side chain is substantially longer than the −CH$_3$ group of pyruvate, leading to more deleterious effects, more specifically, the complete lack of observable ^{13}C-2 polarization in both α-KG isotopologues studied. An additional contribution may arise from coherent leakage from ^{13}C-2 via spin−spin coupling with the nearby protons in protonated systems: at the magnetic fields used, these protons can strongly couple to the ^{13}C-2 site and hence exchange of magnetization could occur.[73,74] Future site-specific hyperpolarization EXSY experiments[75] for determination of dissociation rates in SABRE complexes and computational studies are certainly warranted to support or rule out the presented side chain and coherent leakage hypotheses to explain the presented observations.

The maximum reported P_{13C} values for α-KG and pyruvate in their natural abundance form were 17.3% and 25.5%, respectively, at the time of the detection, and the actual achieved polarization values (inside the apparatus) are likely a few percent higher (the reader is reminded that the produced P_{13C} decays during the sample shuttling from the polarizer to the NMR detector). These values were achieved through rigorous optimization of matching the magnetic field to establish spontaneous polarization transfer and temperature that modulates the rates of simultaneous p-H$_2$ and to-be-hyperpolarized substrate chemical exchange (Figures 2 and 3). While P_{13C} values can be potentially further improved, we anticipate that the gains will likely come from the use of higher p-H$_2$ pressure and flow rates, which have been shown previously to improve access to fresh p-H$_2$, *i.e.*, the source of hyperpolarization.[58,76] The reported studies have been performed at 8 atm, *i.e.*, at the maximum pressure rating for 5 mm NMR tubes employed in our apparatus. Therefore, to achieve these additional potential gains, the design of a specialized hyperpolarizer operating at substantially higher p-H$_2$ pressure and flow rate will be required. Such HP purpose-built setups have been reported for hydrogenative PHIP studies,[26,77−79] and we hope that this report will stimulate the development of corresponding instrumentation for SABRE polarization.

The optimum values of B_T and T_T (and maximum total P_{13C}) for ^{13}C-1 in α-KG isotopologues are nearly identical to those of [1-^{13}C]pyruvate reported recently,[47] indicating that our SABRE-SHEATH polarization transfer approach may be universally tailored to this structural motif of α-ketocarboxylate in other biologically relevant biomolecules, such as [1-^{13}C]α-ketoisocaproate.[80]

The main biomedical limitation of the presented study is the production of the HP substrate in an alcohol-based solution in the presence of an iridium-based catalyst, which may be considered toxic.[81] While the iridium level employed here would likely not impact future feasibility studies in rodents, it would certainly need to be reduced by 2−3 orders of magnitude for clinical use. Several approaches have been

https://doi.org/10.1021/acs.analchem.2c02160
Anal. Chem. 2022, 94, 13422−13431

recently demonstrated to capture an iridium catalyst from SABRE-hyperpolarized solutions.[81−84] Moreover, heterogeneous SABRE approaches have been demonstrated to produce HP compounds free from the catalyst.[85,86] In the context of methanol content of HP samples, it certainly needs to be substantially diluted (or preferably removed completely) for future *in vivo* studies. One way to achieve biocompatible SABRE-based formulation of the HP contrast agent is the use of water-soluble SABRE catalyst approaches, which have also been demonstrated to produce HP compounds in aqueous media to mitigate the use of toxic alcohols.[39,41,43,44] However, the achieved P_{13C} levels using aqueous media have generally been at least an order of magnitude lower than those in methanol (and thus not suitable for in vivo applications, where a high degree of P_{13C} is needed), which has dampened enthusiasm for this approach. The development of biocompatible HP contrast agents' SABRE-based formulations is an active area of research investigations in our partnering and other laboratories, and we anticipate that this report will further stimulate work in that direction.

CONCLUSIONS

In summary, ^{13}C SABRE-SHEATH enables efficient hyperpolarization (P_{13C} of up to 17.3%) of ^{13}C-1 in two α-KG isotopologues: the natural-abundance variant and [1-^{13}C,5-^{12}C,D$_4$]α-KG. [1-^{13}C,5-^{12}C,D$_4$]α-KG is designed as a next-generation molecular probe to sense the real-time metabolism of α-KG *in vivo* using NMR hyperpolarization. This isotopologue is (1) ^{13}C labeled in position 1 for spectroscopic sensing, (2) per-deuterated to maximize the lifetime of the ^{13}C-1 HP state in aqueous media at 3 T, and (3) ^{12}C labeled in position 5 to minimize the background signal from this resonance. Complete deuteration of γ and δ positions has only a minor impact on ^{13}C-1 relaxation in the microtesla fields under our conditions, indicating that spin−spin interactions between ^{13}C-1 and remote proton/deuteron sites and corresponding contributions to ^{13}C-1 relaxation are effectively negligible under these conditions. In contrast, no HP signals from ^{13}C-2 spins were detected from α-KG, and the substantially reduced ^{13}C-2 polarization was detected in the shorter pyruvate molecule; we hypothesize that the binding of the ^{13}C-2 site is generally weaker than that of ^{13}C-1 due to random motion of the side chain (-CH$_3$ in pyruvate and −CH$_2$-CH$_2$-COO- in α-KG). Of critical importance in the context of biomedical utility of HP α-KG as a molecular probe, the SABRE-SHEATH hyperpolarization process leads to highly specific polarization of the ^{13}C-1 site with no detectable polarization on any other sites and most notably ^{13}C-5. This polarization specificity provides a clear benefit over d-DNP, which is a non-site-specific polarization technique and which yields natural-abundance HP ^{13}C-5 α-KG, which overlaps with HP [1-^{13}C]2HG metabolic signal produced via metabolism of HP ^{13}C-1 α-KG in IDH1 mutants.[54] Future systematic experimental and computational binding studies are certainly warranted to obtain a better understanding of relaxation dynamics in these important biomolecules, with the goal to further improve accessible ^{13}C polarization for biomedical applications. We have also presented the feasibility of studying HP substrates at natural ^{13}C abundance (1.1%) using a benchtop NMR spectrometer; indeed, meaningful information is readily obtained at ^{13}C concentrations below 100 μM ^{13}C concentration. The utility of natural-abundance studies in the context of benchtop NMR spectroscopy allows studying a wide range of substrates without ^{13}C isotopic enrichment for ^{13}C SABRE-SHEATH hyperpolarization in a chemistry laboratory without the need for sample transportation to a high-field NMR facility. As a result, we anticipate that the scope of amendable substrates (and laboratories) to SABRE-SHEATH can be rapidly expanded.

ASSOCIATED CONTENT

Supporting Information

The Supporting Information is available free of charge at https://pubs.acs.org/doi/10.1021/acs.analchem.2c02160.

Additional experimental details of SABRE hyperpolarization studies; additional details of synthesis and spectral characterization; additional figures; detailed description of p-H$_2$ storage and distribution system including bill of materials (PDF)

AUTHOR INFORMATION

Corresponding Authors

Jessica Ettedgui − *Chemistry and Synthesis Center, National Heart, Lung, and Blood Institute, Bethesda, Maryland 20850, United States*; Email: jess.benjamini-ettedgui@nih.gov

Rolf E. Swenson − *Chemistry and Synthesis Center, National Heart, Lung, and Blood Institute, Bethesda, Maryland 20850, United States*; Email: rolf.swenson@nih.gov

Eduard Y. Chekmenev − *Department of Chemistry, Integrative Biosciences (IBio), Wayne State University, Karmanos Cancer Institute (KCI), Detroit, Michigan 48202, United States*; orcid.org/0000-0002-8745-8801; Email: chekmenevlab@gmail.com

Authors

Isaiah Adelabu − *Department of Chemistry, Integrative Biosciences (IBio), Wayne State University, Karmanos Cancer Institute (KCI), Detroit, Michigan 48202, United States*

Sameer M. Joshi − *Department of Chemistry, Integrative Biosciences (IBio), Wayne State University, Karmanos Cancer Institute (KCI), Detroit, Michigan 48202, United States*

Shiraz Nantogma − *Department of Chemistry, Integrative Biosciences (IBio), Wayne State University, Karmanos Cancer Institute (KCI), Detroit, Michigan 48202, United States*

Md Raduanul H. Chowdhury − *Department of Chemistry, Integrative Biosciences (IBio), Wayne State University, Karmanos Cancer Institute (KCI), Detroit, Michigan 48202, United States*

Stephen McBride − *Department of Chemistry, North Carolina State University, Raleigh, North Carolina 27695-8204, United States*

Thomas Theis − *Department of Chemistry, North Carolina State University, Raleigh, North Carolina 27695-8204, United States*; orcid.org/0000-0001-6779-9978

Venkata R. Sabbasani − *Chemistry and Synthesis Center, National Heart, Lung, and Blood Institute, Bethesda, Maryland 20850, United States*; orcid.org/0000-0002-4558-2812

Mushti Chandrasekhar − *Chemistry and Synthesis Center, National Heart, Lung, and Blood Institute, Bethesda, Maryland 20850, United States*

Deepak Sail − *Chemistry and Synthesis Center, National Heart, Lung, and Blood Institute, Bethesda, Maryland 20850, United States*
Kazutoshi Yamamoto − *Radiation Biology Branch, Center for Cancer Research, NCI, NIH, Bethesda, Maryland 20892, United States*
Murali C. Krishna − *Center for Cancer Research, National Cancer Institute, Bethesda, Maryland 20814, United States*
Boyd M. Goodson − *School of Chemical & Biomolecular Sciences and Materials Technology Center, Southern Illinois University, Carbondale, Illinois 62901, United States;* orcid.org/0000-0001-6079-5077

Complete contact information is available at: https://pubs.acs.org/10.1021/acs.analchem.2c02160

Notes

The authors declare the following competing financial interest(s): BMG, EYC declare stake ownership in XeUS Technologies, LTD. TT holds stock in Vizma Life Sciences LLC.

■ ACKNOWLEDGMENTS

This work was supported by the NSF under grants CHE-1904780 and CHE-1905341, NIH R21CA220137, and NIBIB R01EB029829. The content is solely the responsibility of the authors and does not necessarily represent the official views of the National Institutes of Health. T.T. also acknowledges funding from the Mallinckrodt Foundation. This research was supported by the Intramural Research Program of the National Cancer Institute and the National Heart, Lung, and Blood Institute, NIH. The content of this publication does not necessarily reflect the views or policies of the Department of Health and Human Services, nor does mention of trade names, commercial products, or organizations imply endorsement by the U.S. Government.

■ REFERENCES

(1) Hoult, D. I.; Richards, R. E. *J. Magn. Reson. (1969)* **1976**, *24*, 71−85.
(2) Blüml, S.; Moreno-Torres, A.; Shic, F.; Nguy, C. H.; Ross, B. D. *NMR Biomed.* **2002**, *15*, 1−5.
(3) Golman, K.; in't Zandt, R.; Thaning, M. *Proc. Natl. Acad. Sci. U.S.A.* **2006**, *103*, 11270−11275.
(4) Day, S. E.; Kettunen, M. I.; Gallagher, F. A.; Hu, D. E.; Lerche, M.; Wolber, J.; Golman, K.; Ardenkjaer-Larsen, J. H.; Brindle, K. M. *Nat. Med.* **2007**, *13*, 1382−1387.
(5) Merritt, M.; Harrison, C.; Storey, C.; Jeffrey, F.; Sherry, A.; Malloy, C. *Proc. Natl. Acad. Sci. U.S.A.* **2007**, *104*, 19773−19777.
(6) Golman, K.; Ardenkjær-Larsen, J. H.; Petersson, J. S.; Månsson, S.; Leunbach, I. *Proc. Natl. Acad. Sci. U.S.A.* **2003**, *100*, 10435−10439.
(7) Kurhanewicz, J.; Vigneron, D. B.; Brindle, K.; Chekmenev, E. Y.; Comment, A.; Cunningham, C. H.; DeBerardinis, R. J.; Green, G. G.; Leach, M. O.; Rajan, S. S.; et al. *Neoplasia* **2011**, *13*, 81−97.
(8) Ardenkjær-Larsen, J. H.; Fridlund, B.; Gram, A.; Hansson, G.; Hansson, L.; Lerche, M. H.; Servin, R.; Thaning, M.; Golman, K. *Proc. Natl. Acad. Sci. U.S.A.* **2003**, *100*, 10158−10163.
(9) Kurhanewicz, J.; Vigneron, D. B.; Ardenkjaer-Larsen, J. H.; Bankson, J. A.; Brindle, K.; Cunningham, C. H.; Gallagher, F. A.; Keshari, K. R.; Kjaer, A.; Laustsen, C.; et al. *Neoplasia* **2019**, *21*, 1−16.
(10) Nikolaou, P.; Goodson, B. M.; Chekmenev, E. Y. *Chem.−Eur. J.* **2015**, *21*, 3156−3166.
(11) Kovtunov, K. V.; Pokochueva, E. V.; Salnikov, O. G.; Cousin, S.; Kurzbach, D.; Vuichoud, B.; Jannin, S.; Chekmenev, E. Y.; Goodson, B. M.; Barskiy, D. A.; et al. *Chem. Asian J.* **2018**, *13*, 1857−1871.
(12) Hövener, J.; Pravdivtsev, A. N.; Kidd, B.; Bowers, C. R.; Glöggler, S.; Kovtunov, K. V.; Plaumann, M.; Katz-Brull, R.; Buckenmaier, K.; Jerschow, A.; et al. *Angew. Chem., Int. Ed.* **2018**, *57*, 11140−11162.
(13) Bowers, C. R.; Weitekamp, D. P. *Phys. Rev. Lett.* **1986**, *57*, 2645−2648.
(14) Eisenschmid, T. C.; Kirss, R. U.; Deutsch, P. P.; Hommeltoft, S. I.; Eisenberg, R.; Bargon, J.; Lawler, R. G.; Balch, A. L. *J. Am. Chem. Soc.* **1987**, *109*, 8089−8091.
(15) Golman, K.; Axelsson, O.; Johannesson, H.; Mansson, S.; Olofsson, C.; Petersson, J. S. *Magn. Reson. Med.* **2001**, *46*, 1−5.
(16) Hövener, J.-B.; Chekmenev, E. Y.; Harris, K. C.; Perman, W.; Robertson, L.; Ross, B. D.; Bhattacharya, P. *Magn. Reson. Mater. Phys.* **2009**, *22*, 111−121.
(17) Goldman, M.; Johannesson, H.; Axelsson, O.; Karlsson, M. *Magn. Reson. Imaging* **2005**, *23*, 153−157.
(18) Cavallari, E.; Carrera, C.; Aime, S.; Reineri, F. *J. Magn. Reson.* **2018**, *289*, 12−17.
(19) Reineri, F.; Boi, T.; Aime, S. *Nat. Commun.* **2015**, *6*, No. 5858.
(20) Knecht, S.; Blanchard, J. W.; Barskiy, D.; Cavallari, E.; Dagys, L.; Van Dyke, E.; Tsukanov, M.; Bliemel, B.; Münnemann, K.; Aime, S.; et al. *Proc. Natl. Acad. Sci. U.S.A.* **2021**, *118*, No. e2025383118.
(21) Zacharias, N. M.; McCullough, C. R.; Wagner, S.; Sailasuta, N.; Chan, H. R.; Lee, Y.; Hu, J.; Perman, W. H.; Henneberg, C.; Ross, B. D.; et al. *J. Mol. Imaging Dyn.* **2016**, *6*, 123.
(22) Bhattacharya, P.; Chekmenev, E. Y.; Reynolds, W. F.; Wagner, S.; Zacharias, N.; Chan, H. R.; Bünger, R.; Ross, B. D. *NMR Biomed.* **2011**, *24*, 1023−1028.
(23) Bhattacharya, P.; Chekmenev, E. Y.; Perman, W. H.; Harris, K. C.; Lin, A. P.; Norton, V. A.; Tan, C. T.; Ross, B. D.; Weitekamp, D. P. *J. Magn. Reson.* **2007**, *186*, 150−155.
(24) Coffey, A. M.; Shchepin, R. V.; Truong, M. L.; Wilkens, K.; Pham, W.; Chekmenev, E. Y. *Anal. Chem.* **2016**, *88*, 8279−8288.
(25) Cavallari, E.; Carrera, C.; Sorge, M.; Bonne, G.; Muchir, A.; Aime, S.; Reineri, F. *Sci. Rep.* **2018**, *8*, No. 8366.
(26) Schmidt, A. B.; Bowers, C. R.; Buckenmaier, K.; Chekmenev, E. Y.; de Maissin, H.; Eills, J.; Ellermann, F.; Glöggler, S.; Gordon, J. W.; Knecht, S.; et al. *Anal. Chem.* **2022**, *94*, 479−502.
(27) Reineri, F.; Cavallari, E.; Carrera, C.; Aime, S. *Magn. Reson. Mater. Phys.* **2021**, *34*, 25−47.
(28) Adams, R. W.; Aguilar, J. A.; Atkinson, K. D.; Cowley, M. J.; Elliott, P. I. P.; Duckett, S. B.; Green, G. G. R.; Khazal, I. G.; Lopez-Serrano, J.; Williamson, D. C. *Science* **2009**, *323*, 1708−1711.
(29) Theis, T.; Truong, M. L.; Coffey, A. M.; Shchepin, R. V.; Waddell, K. W.; Shi, F.; Goodson, B. M.; Warren, W. S.; Chekmenev, E. Y. *J. Am. Chem. Soc.* **2015**, *137*, 1404−1407.
(30) Iali, W.; Roy, S. S.; Tickner, B. J.; Ahwal, F.; Kennerley, A. J.; Duckett, S. B. *Angew. Chem., Int. Ed.* **2019**, *58*, 10271−10275.
(31) Tickner, B. J.; Semenova, O.; Iali, W.; Rayner, P. J.; Whitwood, A. C.; Duckett, S. B. *Catal. Sci. Tech.* **2020**, *10*, 1343−1355.
(32) Barskiy, D. A.; Shchepin, R. V.; Tanner, C. P. N.; Colell, J. F. P.; Goodson, B. M.; Theis, T.; Warren, W. S.; Chekmenev, E. Y. *ChemPhysChem* **2017**, *18*, 1493−1498.
(33) Shchepin, R. V.; Goodson, B. M.; Theis, T.; Warren, W. S.; Chekmenev, E. Y. *ChemPhysChem* **2017**, *18*, 1961−1965.
(34) Zhivonitko, V. V.; Skovpin, I. V.; Koptyug, I. V. *Chem. Commun.* **2015**, *51*, 2506−2509.
(35) Rayner, P. J.; Duckett, S. B. *Angew. Chem., Int. Ed.* **2018**, *57*, 6742−6753.
(36) TomHon, P. M.; Han, S.; Lehmkuhl, S.; Appelt, S.; Chekmenev, E. Y.; Abolhasani, M.; Theis, T. *ChemPhysChem* **2021**, *22*, 2526−2534.
(37) TomHon, P.; Abdulmojeed, M.; Adelabu, I.; Nantogma, S.; Kabir, M. S. H.; Lehmkuhl, S.; Chekmenev, E. Y.; Theis, T. *J. Am. Chem. Soc.* **2022**, *144*, 282−287.
(38) Green, R. A.; Adams, R. W.; Duckett, S. B.; Mewis, R. E.; Williamson, D. C.; Green, G. G. R. *Prog. Nucl. Magn. Reson. Spectrosc.* **2012**, *67*, 1−48.

(39) Shi, F.; He, P.; Best, Q. A.; Groome, K.; Truong, M. L.; Coffey, A. M.; Zimay, G.; Shchepin, R. V.; Waddell, K. W.; Chekmenev, E. Y.; Goodson, B. M. *J. Phys. Chem. C* **2016**, *120*, 12149−12156.
(40) Spannring, P.; Reile, I.; Emondts, M.; Schleker, P. P. M.; Hermkens, N. K. J.; van der Zwaluw, N. G. J.; van Weerdenburg, B. J. A.; Tinnemans, P.; Tessari, M.; Blümich, B.; et al. *Chem.−Eur. J.* **2016**, *22*, 9277−9282.
(41) Truong, M. L.; Shi, F.; He, P.; Yuan, B.; Plunkett, K. N.; Coffey, A. M.; Shchepin, R. V.; Barskiy, D. A.; Kovtunov, K. V.; Koptyug, I. V.; et al. *J. Phys. Chem. B* **2014**, *118*, 13882−13889.
(42) Zeng, H.; Xu, J.; McMahon, M. T.; Lohman, J. A. B.; van Zijl, P. C. M. *J. Magn. Reson.* **2014**, *246*, 119−121.
(43) Hövener, J.-B.; Schwaderlapp, N.; Borowiak, R.; Lickert, T.; Duckett, S. B.; Mewis, R. E.; Adams, R. W.; Burns, M. J.; Highton, L. A. R.; Green, G. G. R.; et al. *Anal. Chem.* **2014**, *86*, 1767−1774.
(44) Colell, J. F. P.; Emondts, M.; Logan, A. W. J.; Shen, K.; Bae, J.; Shchepin, R. V.; Ortiz, G. X.; Spannring, P.; Wang, Q.; Malcolmson, S. J.; et al. *J. Am. Chem. Soc.* **2017**, *139*, 7761−7767.
(45) Eills, J.; Budker, D.; Cavagnero, S.; Chekmenev, E. Y.; Elliott, S. J.; Jannin, S.; Lesage, A.; Matysik, J.; Meersmann, T.; Prisner, T. et al. Spin hyperpolarization in modern magnetic resonance *ChemRxiv* 2022, DOI: 10.26434/chemrxiv-2022-p7c9r.
(46) Ardenkjaer-Larsen, J. H. *J. Magn. Reson.* **2016**, *264*, 3−12.
(47) Adelabu, I.; TomHon, P.; Kabir, M. S. H.; Nantogma, S.; Abdulmojeed, M.; Mandzhieva, I.; Ettedgui, J.; Swenson, R. E.; Krishna, M. C.; Theis, T.; et al. *ChemPhysChem* **2022**, *23*, 131−136.
(48) Tickner, B. J.; Lewis, J. S.; John, R. O.; Whitwood, A. C.; Duckett, S. B. *Dalton Trans.* **2019**, *48*, 15198−15206.
(49) Chapman, B.; Joalland, B.; Meersman, C.; Ettedgui, J.; Swenson, R. E.; Krishna, M. C.; Nikolaou, P.; Kovtunov, K. V.; Salnikov, O. G.; Koptyug, I. V.; et al. *Anal. Chem.* **2021**, *93*, 8476−8483.
(50) Barskiy, D. A.; Kovtunov, K. V.; Koptyug, I. V.; He, P.; Groome, K. A.; Best, Q. A.; Shi, F.; Goodson, B. M.; Shchepin, R. V.; Coffey, A. M.; et al. *J. Am. Chem. Soc.* **2014**, *136*, 3322−3325.
(51) Cowley, M. J.; Adams, R. W.; Atkinson, K. D.; Cockett, M. C. R.; Duckett, S. B.; Green, G. G. R.; Lohman, J. A. B.; Kerssebaum, R.; Kilgour, D.; Mewis, R. E. *J. Am. Chem. Soc.* **2011**, *133*, 6134−6137.
(52) Morris, J. P.; Yashinskie, J. J.; Koche, R.; Chandwani, R.; Tian, S.; Chen, C.-C.; Baslan, T.; Marinkovic, Z. S.; Sánchez-Rivera, F. J.; Leach, S. D.; et al. *Nature* **2019**, *573*, 595−599.
(53) Chaumeil, M. M.; Larson, P. E. Z.; Yoshihara, H. A. I.; Danforth, O. M.; Vigneron, D. B.; Nelson, S. J.; Pieper, R. O.; Phillips, J. J.; Ronen, S. M. *Nat. Commun.* **2013**, *4*, No. 2429.
(54) Miura, N.; Mushti, C.; Sail, D.; AbuSalim, J. E.; Yamamoto, K.; Brender, J. R.; Seki, T.; AbuSalim, D. I.; Matsumoto, S.; Camphausen, K. A.; et al. *NMR Biomed.* **2021**, *34*, No. e4588.
(55) Taglang, C.; Korenchan, D. E.; von Morze, C.; Yu, J.; Najac, C.; Wang, S.; Blecha, J. E.; Subramaniam, S.; Bok, R.; VanBrocklin, H. F.; et al. *Chem. Commun.* **2018**, *54*, 5233−5236.
(56) Vazquez-Serrano, L. D.; Owens, B. T.; Buriak, J. M. *Inorg. Chim. Acta* **2006**, *359*, 2786−2797.
(57) Nantogma, S.; Joalland, B.; Wilkens, K.; Chekmenev, E. Y. *Anal. Chem.* **2021**, *93*, 3594−3601.
(58) Shchepin, R. V.; Truong, M. L.; Theis, T.; Coffey, A. M.; Shi, F.; Waddell, K. W.; Warren, W. S.; Goodson, B. M.; Chekmenev, E. Y. *J. Phys. Chem. Lett.* **2015**, *6*, 1961−1967.
(59) Barskiy, D. A.; Shchepin, R. V.; Coffey, A. M.; Theis, T.; Warren, W. S.; Goodson, B. M.; Chekmenev, E. Y. *J. Am. Chem. Soc.* **2016**, *138*, 8080−8083.
(60) Fekete, M.; Ahwal, F.; Duckett, S. B. *J. Phys. Chem. B* **2020**, *124*, 4573−4580.
(61) Shchepin, R. V.; Birchall, J. R.; Chukanov, N. V.; Kovtunov, K. V.; Koptyug, I. V.; Theis, T.; Warren, W. S.; Gelovani, J. G.; Goodson, B. M.; Shokouhi, S.; et al. *Chem.-Eur. J.* **2019**, *25*, 8829−8836.
(62) Birchall, J. R.; Kabir, M. S. H.; Salnikov, O. G.; Chukanov, N. V.; Svyatova, A.; Kovtunov, K. V.; Koptyug, I. V.; Gelovani, J. G.; Goodson, B. M.; Pham, W.; Chekmenev, E. Y. *Chem. Commun.* **2020**, *56*, 9098−9101.
(63) Bernatowicz, P.; Kubica, D.; Ociepa, M.; Wodyński, A.; Gryff-Keller, A. *J. Phys. Chem. A* **2014**, *118*, 4063−4070.
(64) Blanchard, J. W.; Sjolander, T. F.; King, J. P.; Ledbetter, M. P.; Levine, E. H.; Bajaj, V. S.; Budker, D.; Pines, A. *Phys. Rev. B* **2015**, *92*, No. 220202.
(65) Salnikov, O. G.; Chukanov, N. V.; Svyatova, A.; Trofimov, I. A.; Kabir, M. S. H.; Gelovani, J. G.; Kovtunov, K. V.; Koptyug, I. V.; Chekmenev, E. Y. *Angew. Chem., Int. Ed.* **2021**, *60*, 2406−2413.
(66) Theis, T.; Truong, M.; Coffey, A. M.; Chekmenev, E. Y.; Warren, W. S. *J. Magn. Reson.* **2014**, *248*, 23−26.
(67) Pravdivtsev, A. N.; Skovpin, I. V.; Svyatova, A. I.; Chukanov, N. V.; Kovtunova, L. M.; Bukhtiyarov, V. I.; Chekmenev, E. Y.; Kovtunov, K. V.; Koptyug, I. V.; Hövener, J.-B. *J. Phys. Chem. A* **2018**, *122*, 9107−9114.
(68) Theis, T.; Ariyasingha, N. M.; Shchepin, R. V.; Lindale, J. R.; Warren, W. S.; Chekmenev, E. Y. *J. Phys. Chem. Lett.* **2018**, *9*, 6136−6142.
(69) Tanner, C. P. N.; Lindale, J. R.; Eriksson, S. L.; Zhou, Z.; Colell, J. F. P.; Theis, T.; Warren, W. S. *J. Chem. Phys.* **2019**, *151*, No. 044201.
(70) Pravdivtsev, A. N.; Kempf, N.; Plaumann, M.; Bernarding, J.; Scheffler, K.; Hövener, J.-B.; Buckenmaier, K. *ChemPhysChem* **2021**, *22*, 2381−2386.
(71) Eriksson, S. L.; Lindale, J. R.; Li, X.; Warren, W. S. *Sci. Adv.* **2022**, *8*, No. eabl3708.
(72) Dagys, L.; Bengs, C.; Levitt, M. H. *J. Chem. Phys.* **2021**, *155*, No. 154201.
(73) Gemeinhardt, M. E.; Limbach, M. N.; Gebhardt, T. R.; Eriksson, C. W.; Eriksson, S. L.; Lindale, J. R.; Goodson, E. A.; Warren, W. S.; Chekmenev, E. Y.; Goodson, B. M. *Angew. Chem., Int. Ed.* **2020**, *59*, 418−423.
(74) Chukanov, N. V.; Salnikov, O. G.; Shchepin, R. V.; Svyatova, A.; Kovtunov, K. V.; Koptyug, I. V.; Chekmenev, E. Y. *J. Phys. Chem. C* **2018**, *122*, 23002−23010.
(75) Hermkens, N. K. J.; Feiters, M. C.; Rutjes, F. P. J. T.; Wijmenga, S. S.; Tessari, M. *J. Magn. Reson.* **2017**, *276*, 122−127.
(76) Truong, M. L.; Theis, T.; Coffey, A. M.; Shchepin, R. V.; Waddell, K. W.; Shi, F.; Goodson, B. M.; Warren, W. S.; Chekmenev, E. Y. *J. Phys. Chem. C* **2015**, *119*, 8786−8797.
(77) Schmidt, A. B.; Berner, S.; Schimpf, W.; Müller, C.; Lickert, T.; Schwaderlapp, N.; Knecht, S.; Skinner, J. G.; Dost, A.; Rovedo, P.; et al. *Nat. Commun.* **2017**, *8*, No. 14535.
(78) Agraz, J.; Grunfeld, A.; Li, D.; Cunningham, K.; Willey, C.; Pozos, R.; Wagner, S. *Rev. Sci. Instrum.* **2014**, *85*, No. 044705.
(79) Hövener, J.-B.; Chekmenev, E. Y.; Harris, K. C.; Perman, W.; Tran, T.; Ross, B. D.; Bhattacharya, P. *Magn. Reson. Mater. Phys.* **2009**, *22*, 123−134.
(80) Tickner, B. J.; Ahwal, F.; Whitwood, A. C.; Duckett, S. B. *ChemPhysChem* **2021**, *22*, 13−17.
(81) Manoharan, A.; Rayner, P.; Iali, W.; Burns, M.; Perry, V.; Duckett, S. *ChemMedChem* **2018**, *13*, 352−359.
(82) Barskiy, D. A.; Ke, L. A.; Li, X.; Stevenson, V.; Widarman, N.; Zhang, H.; Truxal, A.; Pines, A. *J. Phys. Chem. Lett.* **2018**, *9*, 2721−2724.
(83) Kidd, B. E.; Gesiorski, J. L.; Gemeinhardt, M. E.; Shchepin, R. V.; Kovtunov, K. V.; Koptyug, I. V.; Chekmenev, E. Y.; Goodson, B. M. *J. Phys. Chem. C* **2018**, *122*, 16848−16852.
(84) Mewis, R. E.; Fekete, M.; Green, G. G. R.; Whitwood, A. C.; Duckett, S. B. *Chem. Commun.* **2015**, *51*, 9857−9859.
(85) Shi, F.; Coffey, A. M.; Waddell, K. W.; Chekmenev, E. Y.; Goodson, B. M. *Angew. Chem., Int. Ed.* **2014**, *53*, 7495−7498.
(86) Kovtunov, K. V.; Kovtunova, L. M.; Gemeinhardt, M. E.; Bukhtiyarov, A. V.; Gesiorski, J.; Bukhtiyarov, V. I.; Chekmenev, E. Y.; Koptyug, I. V.; Goodson, B. M. *Angew. Chem., Int. Ed.* **2017**, *56*, 10433−10437.